Available online at www.sciencedirect.com
ScienceDirect
C. R. Physique 10 (2009) 42–53
COMPTES RENDUS PHYSIQUE

New approaches in Electromagnetic Compatibility / Nouvelles approches en Compatibilité Electromagnétique

Wave chaos techniques to analyze a modeled reverberation chamber

Gérard Orjubin [a,*], Elodie Richalot [b], Odile Picon [b], Olivier Legrand [c]

[a] *Université française d'Egypte, ville de Chorouq, Km 37 autoroute Le Caire-Ismaïlia, B.P. 21, Le Caire, Egypte*
[b] *Université Paris-Est, ESYCOM, EA2552, bâtiment Copernic, 5, boulevard Descartes, 77454 Marne-la-Vallée, France*
[c] *Laboratoire de physique de la matière condensée, CNRS-UMR 6622, Université de Nice-Sophia Antipolis, parc Valrose, 06108 Nice cedex 2, France*

Available online 14 March 2009

Abstract

A Reverberation Chamber (RC) is analyzed with techniques issued from the wave chaos domain. The first 200 modes are determined numerically: their cumulated number is separated into a smooth part, predicted by the Weyl formula, and an oscillating part, interpreted in term of periodic orbits. The technique of the nearest-neighbor spacing distribution is also presented, showing the signature of chaos. Eigenfield distributions are examined for two RC geometries and compared to the Gaussian ideal case. Finally, the notion of avoided crossing is illustrated for an almost chaotic RC, leading to a statement for frequency sweeps induced by the stirrer displacement. ***To cite this article: G. Orjubin et al., C. R. Physique 10 (2009).***

Résumé

Quelques techniques du chaos ondulatoire appliquées à une chambre réverbérante. Une chambre réverbérante (CR) est étudiée grâce à quelques techniques du chaos ondulatoire. Ses 200 premiers modes, déterminés numériquement, permettent de vérifier que la statistique des écarts entre fréquences de résonance voisines dépend du caractère chaotique de la CR, et que les fluctuations du nombre cumulé de modes sont associées aux orbites périodiques. En outre les distributions des champs propres sont étudiées et comparées au cas idéal gaussien pour deux géométries de CR. Enfin la notion de croisement évité est illustrée, propriété des systèmes chaotiques ayant une importante conséquence sur les perturbations provoquées par le brasseur sur les fréquences de résonance. ***Pour citer cet article : G. Orjubin et al., C. R. Physique 10 (2009).***

Keywords: Reverberation chamber; Modal finite element method; Quantum chaos; Electromagnetic cavity

Mots-clés : Chambre réverbérante ; Analyse modale ; Méthode des éléments finis ; Chaos quantique ; Cavité électromagnétique

1. Introduction

Reverberation Chambers (RCs) are used for electromagnetic compatibility tests: they consist of low loss metallic enclosures in which high level electric fields can be generated. In the case of the so-called mechanical stirring, RCs are equipped with a moving metallic insert (the stirrer) that randomizes the ray paths in this highly reflecting environment.

* Corresponding author.
E-mail addresses: orjubin@univ-mlv.fr (G. Orjubin), elodie.richalot@univ-mlv.fr (E. Richalot), odile.picon@univ-mlv.fr (O. Picon), olivier.legrand@unice.fr (O. Legrand).

1631-0705/$ – see front matter
doi:10.1016/j.crhy.2009.01.001

Using statistical electromagnetism, it has been shown [1] that the resulting field inside the RC is homogeneous and isotropic. This proof is based on a plane-wave, integral representation of the fields that is justified in the semiclassic limit where the wavelength is small comparing to RC dimensions. Because they are highly resonant structures, RCs can also be studied using modal expansion [2–4]. We will illustrate that both approaches are closely related to the so-called trace formula first established in the context of quantum mechanics [5, Chapter 7].

Since the 1990s quantum (or wave) chaos theories (semiclassical, Random Matrix Theory) have been validated by electromagnetic experiments with flat cavities [6–8]: in this case there is a one-to-one correspondence between the scalar longitudinal electric field and the scalar wave function given respectively by Helmholtz and stationary Schrödinger equations. More recently three-dimensional (3D) cavities have been studied [9,10]: results tend to prove that vectorial electromagnetic fields follow laws conjectured or proved for scalar wave functions.

The first aim of this article is to extend electromagnetic experiments to RCs, that are particular 3D cavities with an interior conductor. This will be done by comparing predictions of wave chaos theory to some statistics of the eigenmodes (resonant frequencies and the eigenfields) obtained with the modal finite element method (FEM). Although the theory applies to a large number of modes, we will see that the restricted number of analyzed modes (200 modes) is nevertheless enough to assess the chaotic behavior of the RCs according to their geometry. It is worth noting that this paper only concerns the modes of lossless cavities, with neither consideration about the total electric field nor the quality factor, and that the main part of the paper is devoted to the RC analysis at a given stirrer position.

Another objective is to introduce some concepts which might be potentially useful for the Engineering Community, such as the role of chaos in the stirring process or the notion of avoided crossing.

2. Presentation of some wave chaos techniques

2.1. Weyl formula

A lossless electromagnetic cavity (with or without "stirrer") can be described by the set of its real eigenmodes, the eigenvalues corresponding to the resonant frequencies. Let $N(f)$ be the cumulated number of modes whose resonant frequency is inferior to f; then the mean modal density can be expressed [11] as

$$\left.\frac{\mathrm{d}N}{\mathrm{d}f}\right|_{\mathrm{avg}} = \frac{8\pi V}{c}\left(\frac{f}{c}\right)^2 - \frac{\kappa}{c} + o\left[\left(\frac{f}{c}\right)^{-2}\right] \tag{1}$$

where c is the speed of light, V is the enclosure volume and κ is a surface dependent constant. It is notable that the equivalent at high frequency depends on the cavity volume but not on the boundary surface: it is therefore independent of the thin stirrer. Within this approximation one gets the Weyl formula

$$N_{\mathrm{Weyl}}(f) = \frac{8\pi V}{3}\left(\frac{f}{c}\right)^3 \tag{2}$$

It is also possible to express a Generalized Weyl formula from (1). For a stirrerless rectangular cavity of dimensions (L_x, L_y, L_z) it comes [11]

$$N_{\text{Generalized Weyl}}(f) = \frac{8\pi V}{3}\left(\frac{f}{c}\right)^3 - (L_x + L_y + L_z)\frac{f}{c} + \frac{1}{2} \tag{3}$$

A direct calculation of $N(f)$ for this integrable problem has proved [12] that (3) corresponds to local average of $N(f)$. This property is general: the Generalized Weyl formula gives the smooth evolution with frequency of the number of modes. We will see in the next paragraph that fluctuations between this mean value and the actual number of modes can be interpreted using a semiclassical approach.

2.2. Semi-classical approach, trace formula

In Geometric Optics, rays propagate freely inside the RC until they are reflected from boundaries. Because this is the analogue to the trajectory of a particle free to move in a hard wall enclosure (billiard), the so-called semiclassical approach is based on concepts developed for mechanics. For example a special attention is paid to periodic orbits

(POs), which are closed trajectories in the phase space, as their properties yield a classification of the underlying dynamical system into integrable or chaotic [13].

One of the most important results regarding the semiclassical approach is the "trace formula" that establishes the correspondence between modal properties and the ray model. It has been first demonstrated for quantum chaos theory [5, Chapter 7], and then for electromagnetic problems [14,15]. It is shown that modal fluctuations around the mean modal density (1) have an oscillatory behavior

$$\frac{\mathrm{d}N}{\mathrm{d}f} = \left.\frac{\mathrm{d}N}{\mathrm{d}f}\right|_{\mathrm{avg}} + \sum_i A_i \mathrm{e}^{j\frac{2\pi f}{c}L_i} \tag{4}$$

where L_i is the length of the ith PO.

As the Fourier Transform of the fluctuating part, called length spectrum, is a sum of Dirac, one can determine the length L_i of the first POs from a resonant frequencies study.

2.3. Random Matrix Theory, distribution of resonant frequencies

Spectral fluctuations can be statistically described using Random Matrix Theory (RMT) [5, Chapter 3]. According to a conjecture that has been checked for various domains of Physics, the nearest-neighbor spacing distribution (obtained from n consecutive resonant frequencies) depends on the symmetry of the underlying system (chaotic or integrable, with or without losses), but not on its geometry. To exhibit such "universal" behavior, the spectrum has to be unfolded by the following procedure.

After sorting the $\{f_1, f_2, \ldots, f_n\}$ resonant frequencies, the actual cumulated number of modes $N(f)$ is plotted and fitted to a third order polynomial $N_{\mathrm{avg}}(f)$ that corresponds to the smooth part of $N(f)$. Instead of analyzing the fluctuation $N(f) - N_{\mathrm{avg}}(f)$ using (4), the technique employed here consists of determining the normalized spacings between eigenfrequencies

$$s_i = N_{\mathrm{avg}}(f_{i+1}) - N_{\mathrm{avg}}(f_i) \tag{5}$$

Then the empirical distribution of s is compared to theoretical distributions conjectured by RMT: For a lossless integrable system (e.g. a parallelepiped cavity without stirrer) the probability density function $P(s)$ is exponential

$$P(s) = \mathrm{e}^{-s}, \quad s \geqslant 0 \tag{6}$$

For most lossless chaotic systems (e.g. an RC with complex shaped stirrer) frequency spacings follow the Wigner law (special case of Rayleigh distribution) expressed as

$$P(s) = \frac{\pi}{2} s \mathrm{e}^{-\frac{\pi}{4}s^2}, \quad s \geqslant 0 \tag{7}$$

These two probability density functions (pdfs) and cumulated density functions (cdfs) are plotted in Fig. 1.

Fig. 1(a) illustrates the "level repulsion" phenomenon $P(s = 0) = 0$ for Wigner pdf: the probability of two modes to be degenerated is null for chaotic systems. This property is reflected in the slope at cdf's origin in Fig. 1(b). Not only small spacings but also larger ones are fewer: in other words frequency spacings are more concentrated around their mean value for a chaotic system. Conversely for integrable systems modal degeneracy and clustering are favored because the exponential pdf is peaked at $s = 0$.

Attention has to be drawn to the fact that this theory relies on two important hypotheses: first the modes under investigation should be asymptotic (high frequency limit), secondly the wave equation under consideration should be scalar. However, we will see that processing the first 200 eigenfrequencies of an RC yields statistics fairly in agreement with RMT predictions, even for this 3D electromagnetic problem.

2.4. Eigenfield distribution

It is well known that each mode of a 3D rectangular cavity (without stirrer) is a sum of eight plane waves [12]. The plane wave decomposition was generalized as a random plane wave model by Berry [16] in quantum chaos context, them by Hill [1] for RCs. It consists of expanding the modes of a given enclosure into a continuous sum of plane waves (i.e. rays) whose wave vector is arbitrarily oriented but with the same amplitude. Within this assumption, the central limit theorem indicates that eigenfield spatial distributions are Gaussian.

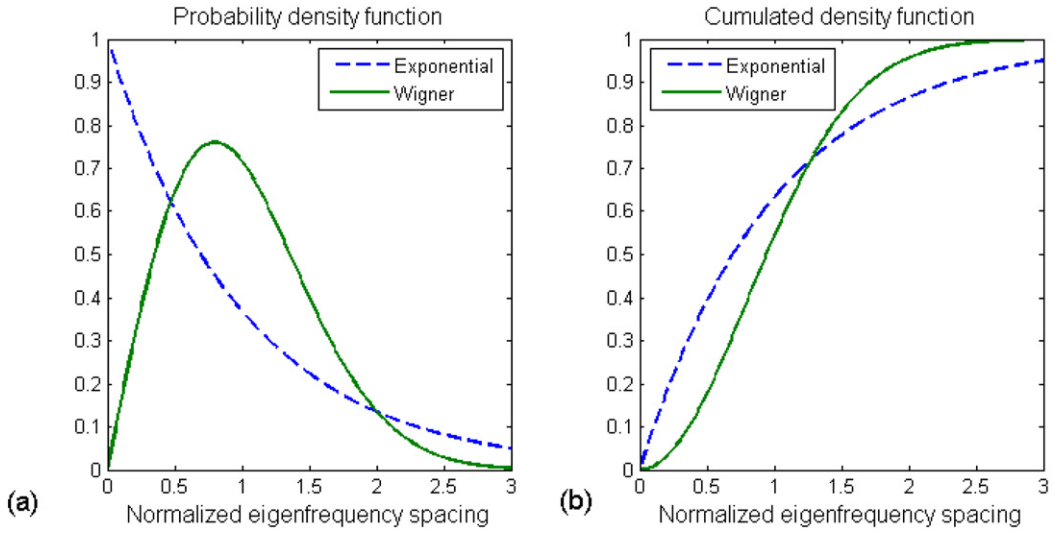

Fig. 1. Probability (a) and cumulated (b) density functions for exponential and Wigner types.

Fig. 1. Densité de probabilité (a) et fonction de répartition (b) des lois exponentielle et de Wigner.

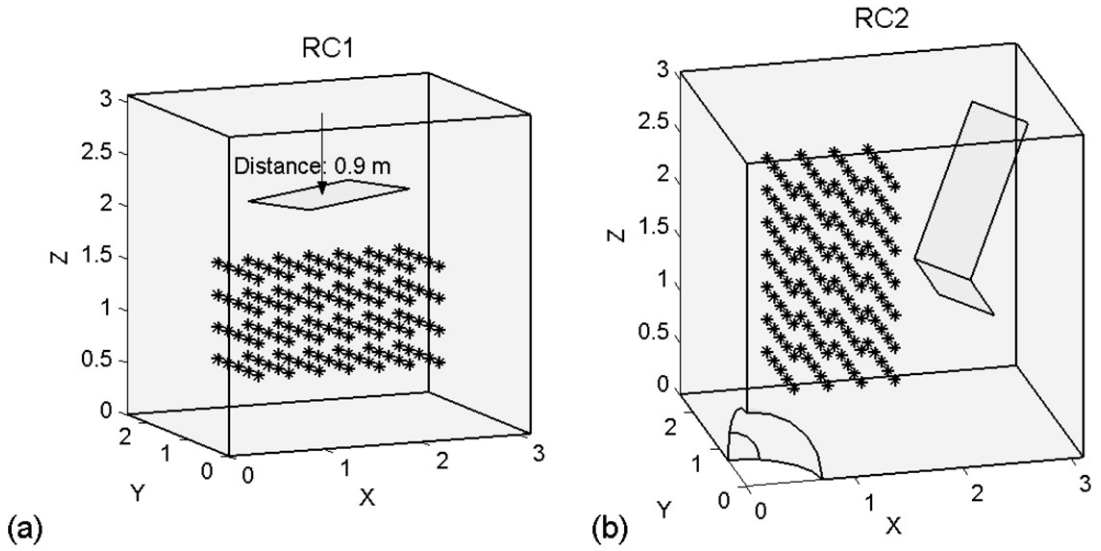

Fig. 2. Studied RCs with the 140 points (*) where fields are evaluated in Section 3.5. (a) RC1. (b) RC2.

Fig. 2. CRs étudiées avec les 140 points (*) où sont évalués les champs dans le Section 3.5. (a) CR1. (b) CR2.

3. Application to RCs

The techniques presented in the previous paragraphs are applied to study two RCs represented in Fig. 2, both of them being built from a same rectangular cavity whose dimensions in meters are $(L_x, L_y, L_z) = (3.10, 2.47, 3.07)$. RC1 is a rectangular cavity with a basic plane rectangular stirrer of dimensions 0.75 m × 1.5 m placed at 0.9 m from the roof. RC2 features a V-folded stirrer (0.75 m width, total length 1.5 m + 0.5 m), in a Sinai-type cavity (this kind of cavity is studied in [10]). We remind that rectangular cavities are integrable and Sinai-type cavities are fully chaotic leading to different spectral and spatial statistics as mentioned above. Therefore we expect RC2 to follow properties of chaotic systems and RC1 to be in the grey-zone between the integrable and chaotic cases.

The study begins with a determination of the first RC modes at a given stirrer position.

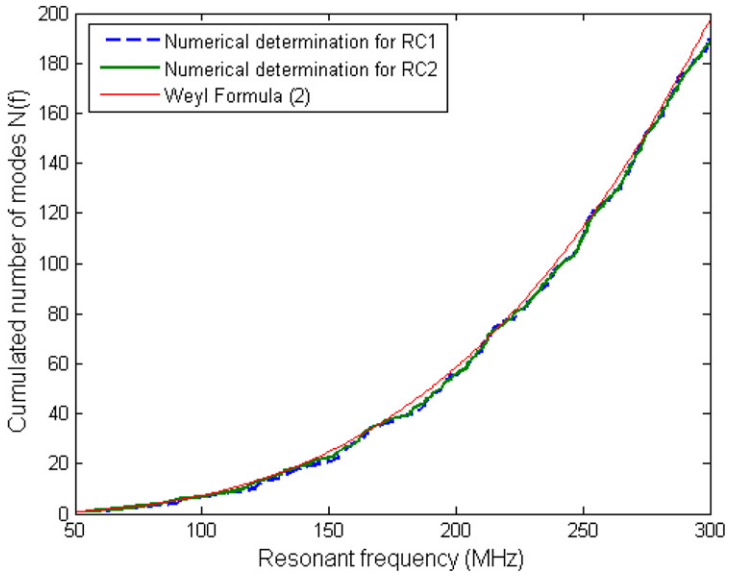

Fig. 3. RC1 and RC2 cumulated number of modes obtained by finite element method.

Fig. 3. Nombre cumulé de modes de CR1 et CR2 obtenus par la méthode des éléments finis.

3.1. Numerical determination of the modes

FEM enables a direct determination of the modes as lossless RC modeling leads to a generalized eigenvalue problem for which efficient solvers exist. We chose the Jacobi–Davidson algorithm implemented in the open source program Pysparse [4] for its capability to compute a large number of consecutive modes. To find N eigenvalues of this high dimensional problem whose dimension is equal to the number of degrees of freedom (#DoF), the method is based on a projection onto a subspace whose dimension increases iteratively up to $2N$. As we investigate the distribution of N eigenmodes, N has to be as large as possible within the constraint of the memory space necessary to process sparse matrices of dimension #DoF. As a trade-off between the accuracy of numerical determination of the higher rank modes (related to #DoF) and the number of modes used to validate wave chaos theory, N is set to 200.

The RC volume is meshed with tetrahedra of maximum edge length 0.2 m, corresponding to a fifth of the shorter wavelength (@300 MHz). In order to enhance the precision of the electric field determination, a refined mesh is imposed on the stirrer with triangles of dimensions smaller than 0.1 m. Although second order elements bring a clear advantage over first order elements (Nédélec) in term of accuracy, the latter are used to save memory space. Finally it takes a reasonable 4.5×10^3 s (Pentium IV, 3.2 GHz) to solve the numerical problem for $N = 200$ and 60×10^3 DoFs.

3.2. Weyl formula

Consecutive resonant frequencies are given directly by the solver: their empirical cumulative number is plotted in Fig. 3 and is compared to the Weyl formula (2).

Although (2) is only applicable for stirrerless rectangular cavities, it provides a good estimation of $N_{\text{avg}}(f)$ for RC1 and RC2, without sophisticated calculation of the surface term κ for this double connected system.

3.3. Length spectrum

As explained in Section 2.2 fluctuations of modal density are related to PO lengths. To illustrate this point the fluctuation part is estimated by the difference between the actual $N(f)$ and the approximation (2). Fig. 4(a) shows that the fit is biased, principally because (2) is not really indicated for these complex cavities, and secondly because FEM introduces numerical errors increasing with frequency.

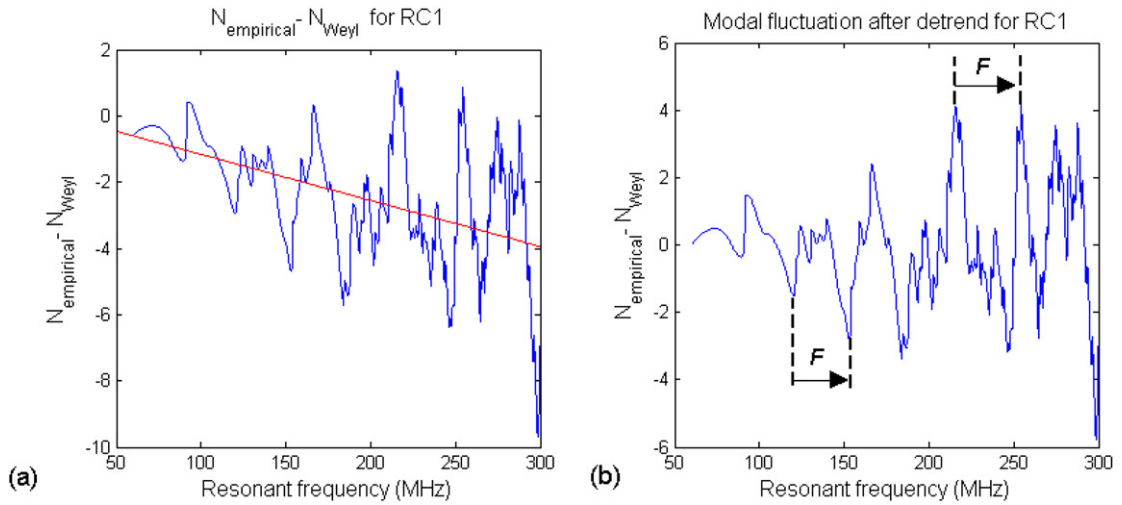

Fig. 4. Fluctuations of RC1 cumulated number of modes. Before (a) and after (b) detrending.

Fig. 4. Fluctuations du nombre cumulé de modes de CR1 avant (a) et après (b) suppression de tendance.

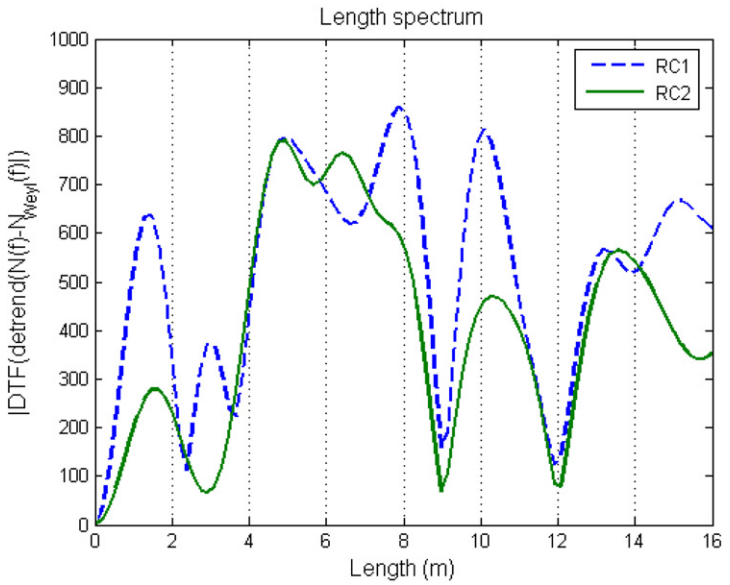

Fig. 5. Length spectrum for RC1 and RC2.

Fig. 5. Spectres de longueur de CR1 et CR2.

After eliminating this linear trend, one gets in Fig. 4(b) the spectral fluctuations of $N(f)$ that present some periodic behaviors. For instance a $F \approx 30$ MHz period can be noticed: in the transformed domain, the oscillation will appear as a peak centralized at $L = c/F = 10$ m. This is confirmed by the length spectrum obtained by Discrete Fourier Transform (DFT) of these fluctuations (see Fig. 5).

The peaks of the length spectrum are situated at the lengths L_i of the POs. For both RCs we find in Fig. 5 evidences of the "bouncing-ball" orbits of length $2L_y = 4.95$ m and $4L_y$ that bounce back and forth between the two parallel lateral surfaces distant by L_y. We also notice for RC1 that the second peak is located at 3.6 m, i.e. 4 times the distance between the stirrer and the RC top (see Fig. 2(a) where this PO is represented).

Caution must be taken when interpreting the first peak at 1.8 m. Although this length corresponds to the first PO situated above the stirrer of RC1, a parametric study (with the height of the stirrer) proves that this peak has

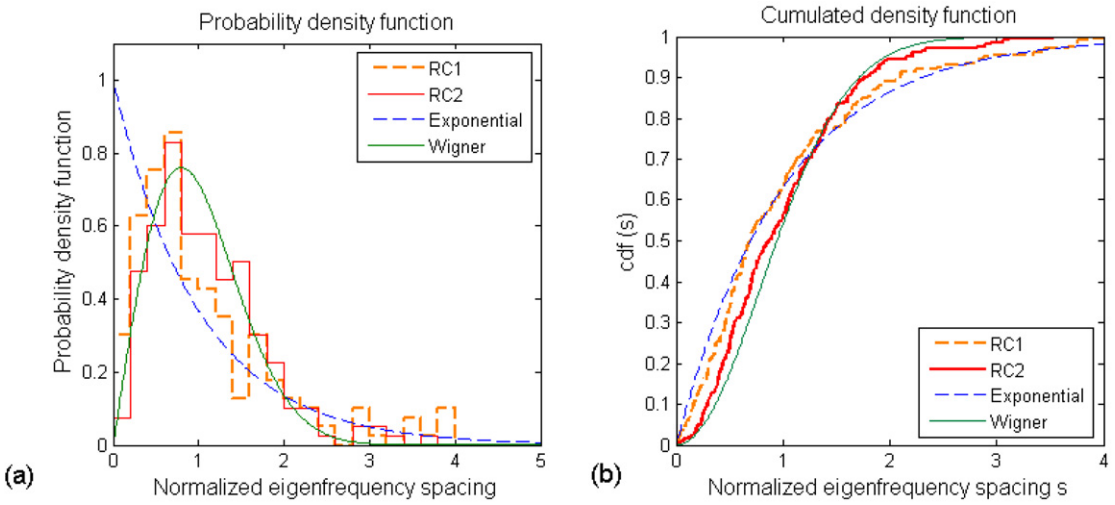

Fig. 6. Pdf (a) and cdf (b) of the RC nearest neighbor frequency spacing obtained by FEM modeling.

Fig. 6. Densité de probabilité (a) et fonction de répartition (b) des distributions obtenues par FEM des écarts entre fréquences adjacentes.

no physical origin. In fact, $L = 1.8$ m is associated to a 167 MHz period in the original domain $N(f)$. A visual inspection at Fig. 4(b) suggests that the DFT of this large period signal will present some windowing artifact. To reduce this effect and improve the resolution, the number of studied modes should be larger than 200. For instance a much better resolution is obtained in [17] from the study of 18,764 modes.

3.4. Nearest-neighbor spacing distribution

After analyzing modal density fluctuation, we study now the normalized spacings between two consecutive resonant frequencies, as suggested by RMT. In order to calculate the s_i parameter (5), the curves shown in Fig. 3 are approximated by a third order polynomial representing $N_{\text{avg}}(f)$. Then a histogram is created from empirical data (Fig. 6(a)).

In Fig. 6 level repulsion is clearly shown for RC2, in agreement with theory for this chaotic enclosure. Without surprise empirical cdfs obtained from 200 modes do not match perfectly to RMT prediction (that supposes that the number of modes is infinite). However we notice that empirical distributions are very different one to the other, being as well quite close to theoretical cdfs. As the basic stirrer of RC1 does not change significantly the symmetry of this integrable cavity, the cdf is close to an exponential law. On another hand, a complex stirrer in a Sinai-type cavity makes RC2 a chaotic system for which the spacings s follow a Wigner-like distribution. Therefore s statistics reveal the chaotic nature of the cavity, even for these mixed systems. As an application, the difference between Wigner and empirical cdfs can be exploited as a metric of chaoticity [18].

3.5. Eigenfield distribution

The solver provides the real eigenfields associated to resonant frequencies. In order to check if these eigenvector spatial distributions are Gaussian, fields are projected on a grid whose spacings in the directions x, y and z are respectively $L_x/10$, $L_y/10$ and $L_z/10$, i.e. roughly 0.30 m. Because data must be uncorrelated, the spatial spacing must be larger than a quarter of a wavelength [19, Annex B, Note 5]: only modes of rank higher than 100 are kept (their frequency is $f > 242$ MHz). Also, grid points close to boundaries by less than 0.5 m are discarded. Finally for each mode and each rectangular component $E_R = E_{x,y,z}$ an histogram is constructed from the E_R values at 140 points pictured in Fig. 1. Besides, the medium sized data set, we notice in Fig. 7 clear differences from mode to mode.

A quantitative investigation is performed to determine the proportion of modes that are normally distributed. The Shapiro–Wilk goodness-of-fit test is used [20], with the following convention: the result of the test is 0 if the null

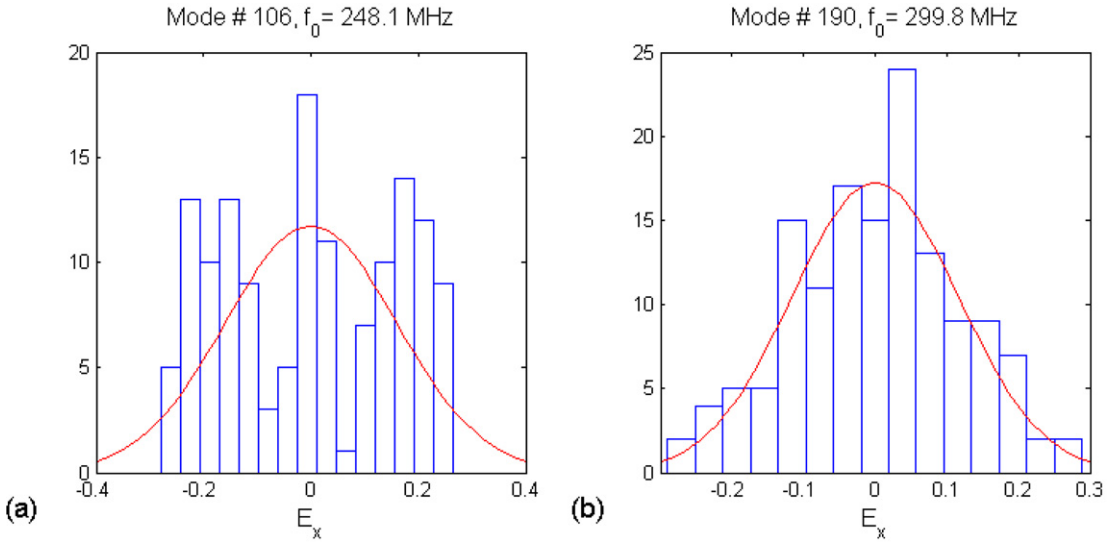

Fig. 7. Histograms of the 140 E_x values for the RC1 modes ranked 106 and 190.

Fig. 7. Histogrammes des 140 valeurs de E_x pour les modes de rang 106 et 190, CR1.

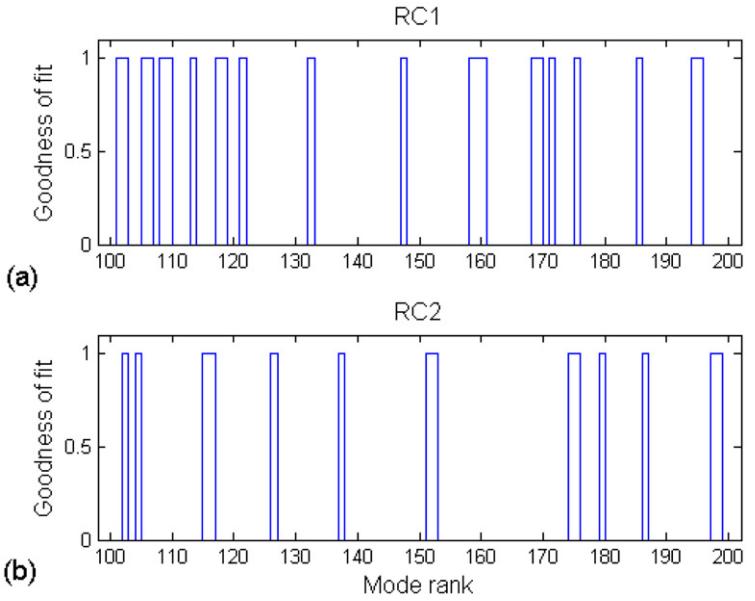

Fig. 8. Shapiro–Wilk normality test for E_x, mode ranks between 100 and 200. Result is 0 if E_x is considered as Gaussian.

Fig. 8. Test de normalité de Shapiro–Wilk pour E_x, rang des modes entre 100 et 200. Le résultat est 0 lorsque E_x est considéré comme gaussien.

hypothesis of normality is accepted, 1 if it is rejected at 5% significance level. For the modes of rank 106 and 190 analyzed in Fig. 7, the result is 1 and 0 respectively. Then the results for all E_x components are graphed in Fig. 8.

Fig. 8 shows that E_x components (modes rank from 100 to 200) are more likely to obey a Gaussian law for RC2 rather than for RC1. This is confirmed by the mean success rate indicated in Table 1.

As the significance level is 5%, the Gaussian hypothesis is not strictly accepted for modes of rank lower than 200. Nevertheless information contained in Table 1 can be exploited as a metric of RC performances: For instance RC2 modes have distributions closer to Gaussian than the ones of RC1, a fact that can be attributed to the stirrer shape and the cavity type.

Table 1
Mean success rate for normality test for modes with rank between 100 and 200 (i.e. frequency between 242 and 300 MHz).

Tableau 1
Taux de réussite moyen au test de normalité pour les modes de rangs entre 100 et 200 (soit une fréquence entre 242 et 300 MHz).

	E_x	E_y	E_z
RC1	0.22	0.29	0.44
RC2	0.14	0.23	0.19

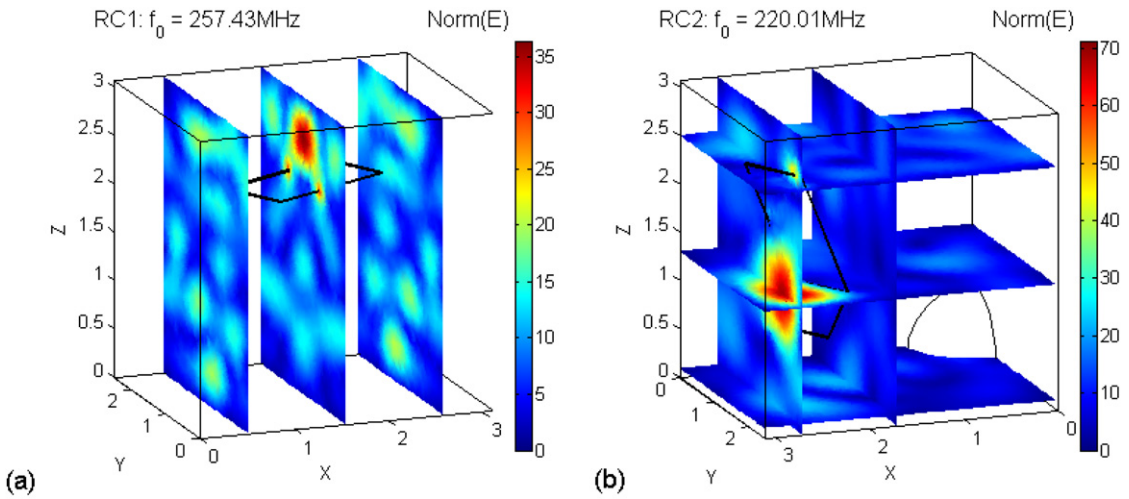

Fig. 9. Examples of non-generic modes. (a) Mode rank 110 for RC1. (b) Mode rank 77 for RC2.

Fig. 9. Exemples de modes non génériques. (a) Mode de rang 110 pour CR1. (b) De rang 77 pour CR2.

3.6. Examples of cartographies

Apart from the generic modes of a chaotic system which are normally distributed, some special modes presenting spatial localization exist. This is shown in Fig. 9 for RC1 and RC2.

In Fig. 9(a) we notice that the mode (rank 110) is situated above the stirrer along the PO whose length has been determined in Fig. 5 as a consequence of the trace formula. A similar phenomenon can be observed in Fig. 9(b): the mode is localized in the neighborhood of a PO that bounces between the stirrer and the cavity corner.

The previous modes belong to families that are intensively studied for two-dimensional (2D) billiards [7], and sometimes for 3D cavities [10]. Besides the fact that these modes present hot spots that could have dramatic consequences for RC applications, it is worth noting that the total field averages eventual localizations as it is a sum over many modes.

4. Perturbation of the resonant frequencies

Eigenmode distributions were investigated in Section 3 at a given stirrer position. In this section we consider the effect of the stirrer rotation on the resonant frequencies. This kind of study, which contributes to a better understanding of the stirring process, has been initiated by Wu and Chang [21] for a TLM model of a 2D RC. In that case eigenvalues are obtained indirectly: first TLM provides a time domain response, then a Fourier Transform gives the frequency response, and finally the resonant frequencies are associated to the maxima of that response. Because of implicit time windowing, this technique resolution is limited and frequency separation is uneasy for nearly degenerated modes. This drawback does not exist for modal FEM determination: as the solver finds all the modes even if degenerated,

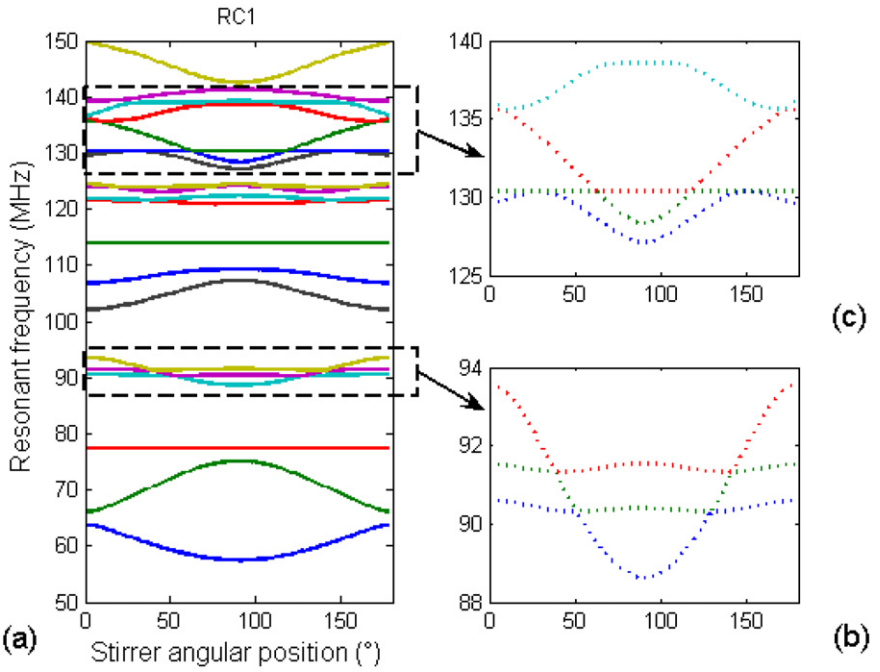

Fig. 10. Resonant frequencies of the 20 first modes of RC1, for a stirrer rotation.

Fig. 10. Relevé des 20 premières fréquences de résonance pour une rotation du brasseur de CR1.

modal FEM is well indicated to track the modes during a stirrer displacement. To reduce numerical errors, the #DoF is increased to 200×10^3 using second order elements. It takes some 1500 s to find the first 20 modes, this calculation being reiterated at each step of the stirrer displacement (2° rotation around a vertical axis passing by the stirrer center).

The RC1 resonant frequencies are plotted in Fig. 10 as functions of the stirrer position.

Fig. 10 shows that the stirrer rotation does not increase the number of modes, as expected according to the Weyl formula, and produces frequency shifts, as observed experimentally. For a complete stirrer rotation, the resonant frequencies perturbations are periodic, some of the modes being undisturbed by the particularly simple RC1 stirrer (e.g. the third mode at frequency 77 MHz is TM_{110}). Of great interest is the case of the modes ranked 4–6: Although the solver gives sorted resonant frequencies, a careful inspection of the zoom given in Fig. 10(b) suggests that crossings occur between the curves, phenomenon also observed in Fig. 10(c) for higher rank modes. As a comparison, RC2 results are graphed in Fig. 11.

We notice that all RC2 modes are affected by the stirrer and that no crossing occurs. In some cases (e.g. mode numbers 7, 8) curves get close but crossing is avoided. This is another illustration of the level repulsion inherent to chaotic system: as $P(s = 0) = 0$ for Wigner distribution, the probability to have degenerate modes vanishes.

As there are no crossings for chaotic systems, an analogy can be made between the evolution of the resonant frequencies and the particle movements in a one-dimensional gas [5, Chapter 5]. The quantum chaos Community investigates eigenvalue perturbations referring to “level dynamics”, and studies concern distributions of eigenvalue velocities or avoided crossings.

Although these considerations seem very far from the RC application, we can concentrate on the property stating that crossings are avoided for chaotic systems. This means that frequency sweeps induced by the stirrer displacement are bounded by the spacings to nearest neighbors. Then the mean frequency sweep is inferior to the mean spacing between eigenvalues. As modal density varies with f^2 (see Eq. (1)), the mean spacing between resonant frequencies vanishes at high frequencies. Consequently the stirrer induced resonant frequency shifts whose amplitudes tend to zero at high frequency.

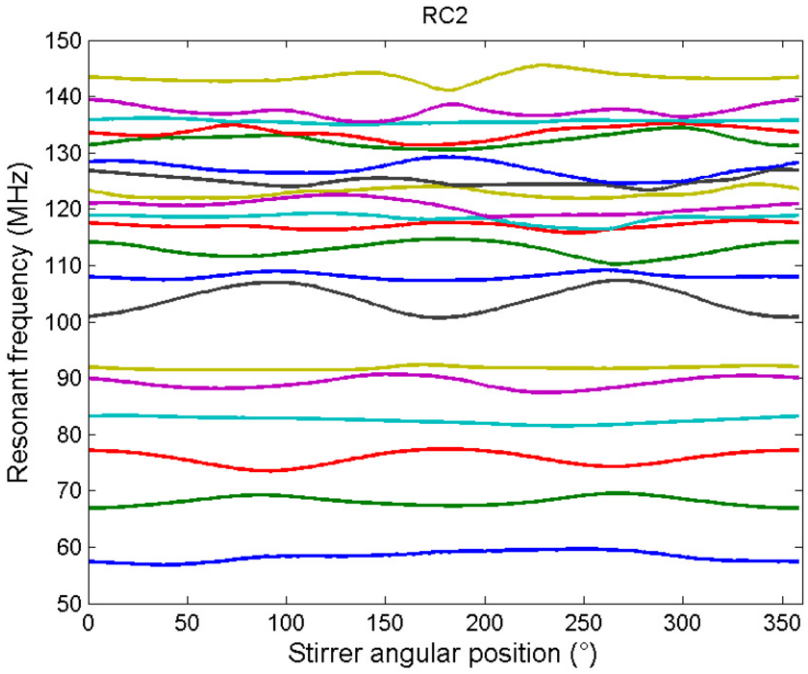

Fig. 11. Evolution of RC2 resonant frequencies with stirrer position.

Fig. 11. Evolution des fréquences de résonance de RC2 en fonction de la position du brasseur.

5. Conclusion

Microwave experiments with flat cavities are recognized to enable macroscopic validation of quantum chaos theory. Despite some differences due to the vector nature of electromagnetic fields, this approach is successfully extended to 3D electromagnetic cavities by some authors. We check in this paper that reverberation chambers (RCs), as a special kind of cavity, follow general results.

In this aim two RCs (from very basic to realistic) are modeled by finite element method. The modes are first determined at a given stirrer position. It is checked that the Weyl formula gives a good approximation of the smooth variation with frequency of the cumulative number of modes. Then fluctuations of the modal density are investigated using the trace formula. The correspondence between the modal and semiclassic approaches is illustrated by the length determination of some periodic orbits. Next, statistical studies of 200 eigenmodes (resonant frequency spacing and eigenfield) validate the RMT conjecture: for a complex shaped RC, empirical distribution functions are close to the theoretical ones predicted for lossless chaotic systems, despite the small number of studied modes.

Following this conceptual approach, a better knowledge of the RC is gained. The importance of RC chaoticity is explained for the distributions of eigenmodes: resonant frequencies have more regular spacings, avoiding clustering, and eigenfields are more likely to be spatially Gaussian, contributing to the total field homogeneity. Finally an important property is given concerning the issue of frequency sweep induced by the stirrer rotation in a chaotic RC.

Acknowledgements

This work was supported by the CNPq and FUNCAP Brazilian agencies.

References

[1] D.A. Hill, Plane wave integral representation for fields in reverberation chambers, IEEE Trans. Electromag. Compat. 40 (1998) 209–217.
[2] C.F. Bunting, et al., A two-dimensional finite-element analysis of reverberation chambers, IEEE Trans. Electromag. Compat. 41 (1999) 280–289.

[3] G. Cerri, et al., Investigation of the antenna factor behavior of a dipole operating inside a resonant cavity, IEEE Trans. Electromag. Compat. 50 (2008) 89–96.
[4] G. Orjubin, et al., On the FEM modal approach for a reverberation chamber analysis, IEEE Trans. Electromag. Compat. 49 (2007) 76–85.
[5] H.-J. Stöckmann, Quantum Chaos. An Introduction, Cambridge University Press, Cambridge, 1999.
[6] H.J. Stöckmann, J. Stein, Quantum chaos in billiards studied by microwave absorption, Phys. Rev. Lett. 64 (1990) 2215–2218.
[7] S. Sridhar, Experimental observation of scarred eigenfunctions of chaotic microwaves cavities, Phys. Rev. Lett. 67 (1991) 785–788.
[8] J. Barthélemy, O. Legrand, F. Mortessagne, Complete S matrix in a microwave cavity at room temperature, Phys. Rev. E 71 (2005) 016205.
[9] S. Deus, P.M. Koch, L. Sirko, Statistical properties of the eigenfrequency distribution of the three-dimensional microwave cavities, Phys. Rev. E 52 (1995) 1146–1155.
[10] U. Dörr, et al., Scarred and chaotic field distributions in a three-dimensional Sinai microwave resonator, Phys. Rev. Lett. 80 (1998) 1030–1033.
[11] L.R. Arnaut, Operation of electromagnetic reverberation chambers with wave diffractors at relatively low frequencies, IEEE Trans. Electromagn. Compat. 43 (2001) 637–653.
[12] B.H. Liu, D.C. Chang, M.T. Ma, Eigenmodes and the composite quality factor of a reverberating chamber, Nat. Bur. Stand. (U.S.) (1983), Tech. Note 1066.
[13] V. Galdi, I.M. Pinto, L.B. Felsen, Wave propagation in ray-chaotic enclosures: Paradigms, oddities and examples, IEEE Antennas and Propagation Magazine 47 (2005) 62–81.
[14] R. Balian, B. Duplantier, Electromagnetic waves near perfect conductors. I. Multiple scattering expansions. Distribution of modes, Ann. Phys. 104 (1977) 300–335.
[15] H.P. Baltes, Asymptotic eigenvalue distribution for the wave equation in a cylinder of arbitrary cross section, Phys. Rev. A 6 (1972) 2252–2257.
[16] M.V. Berry, Regular and irregular semiclassical wavefunctions, J. Phys. A 10 (1977) 2083–2091.
[17] C. Dembowski, et al., Experimental test of a trace formula for a chaotic three-dimensional microwave cavity, Phys. Rev. Lett. 89 (2002) 064101.
[18] G. Orjubin, et al., Chaoticity of a reverberation chamber assessed from the analysis of modal distributions obtained by FEM, IEEE Trans. Electromag. Compat. 49 (2007) 732–771.
[19] IEC 61000-4-21 Electromagnetic Compatibility: Reverberation Chamber Test Methods, Intern. Electrotech. Commission (IEC), Geneva, 2003.
[20] J.P. Royston, An extension of Shapiro and Wilk's W test for normality to large samples, Appl. Statist. 31 (1982) 115–124.
[21] D.I. Wu, D.C. Chang, The effect of an electrically large stirrer in a mode-stirred chamber, IEEE Trans. Electromag. Compat. 31 (1989) 164–169.